

# Resin-Based Copper-Free Brake Pads: A Right Selection of Potassium Titanate and Ceramic Fiber

Hamid Ansari Moghadam<sup>1,\*</sup>, Saeed Banaeifar<sup>2</sup>, Reza Tavangar<sup>3</sup>, Ali Reza Khavandi<sup>1</sup>, Soheil Mahdavi<sup>3</sup>

\* Hamid\_ansari@metaleng.iust.ac.ir

<sup>1</sup> School of Metallurgy and Materials Engineering, Iran University of Science and Technology, Tehran, Iran

<sup>2</sup> School of Metallurgy and Materials Engineering, University of Tehran, Tehran, Iran

<sup>3</sup> Faculty of Materials Engineering, Sahand University of Technology, Tabriz, Iran

Received: June 2021

Revised: November 2021

Accepted: December 2021

DOI: 10.22068/ijmse.2320

**Abstract:** The present study was aimed to assess the effect of replacing copper in the brake pad with potassium titanate platelet (PTP) and ceramic fiber (CF). Chase dynamometer tests were conducted to compare a brake pad's tribological behavior when PTP and CF are added to the composition with that of the copper-bearing pad. The results indicated that PTP and CF demonstrated promising outcomes such as a stable coefficient of friction (COF), lower wear rate, and better heat resistance in copper-free friction composite. Scanning electron microscope (SEM/EDS) analysis was conducted to investigate the role of main elements such as Ti, Fe, K, O, and C on the formation of contact plateaus of friction composites. PTP maintained both continuous contact and smooth friction braking application of a brake pad. The uniform distribution of Ti on the wear track on the worn surface depicts the role of PTP in stabilizing the friction film formation.

**Keywords:** copper-free, potassium titanate, ceramic fiber, brake pad, friction materials.

## 1. INTRODUCTION

Brake pad polymer matrix composite for today's vehicles is a complex combination of different materials that provide the expected properties during brake applications. Herbert Froot who began developing friction material composites (FMCs) and used a wooden brake block machined to fit within a metal holder [1]. Over time, the friction composite ingredients developed to meet the requirements for high-performance brake pads and, more specifically, the legislation's changes for some forbidden materials that harm the environment and humans. Generally, tribological brake pad and lining composites comprise ceramic matrix composite, metallic matrix composite, and polymer matrix composite. The polymer matrix composite is also known as resin-based friction composite [2], and it is the most commonly used among friction composites due to its ease of fabrication. Commonly used resin-based FMC was categorized into three classes: metallic, low-metallic, and Non-Asbestos Organic (NAO) FMCs [3]. All polymer matrix formulations consist of four core material categories: binder, friction modifiers (lubricants, abrasives), reinforcements, and fillers [4]. Depending on the desired characteristics of brake pads, the formulation undergoes some changes in

the use of the functional ingredients.

Copper-Free friction composite is one of the latest friction formulations that many researchers and manufacturers have attempted to develop as the environmental concerns have led to legislation that forced the manufacturers to comply with the obligation of using copper within the formulation less than 0.5% by 2025. This situation created some challenges for replacing copper with new ingredients being able to play the role of copper to keep its multi-functional properties unchanged or even improve (i) stable coefficient of friction (COF) (ii) good wear and fade resistance (sudden decrease of COF at the elevated temperature called fade) (iii) good stability during service at high temperature and (iv) eliminate noise in braking [5].

Copper is mostly referred to as a friction modifier in the friction composite [6–9] and acts as a high-temperature lubricant [10] that brings about a smoother sliding surface resulting in reducing noise generation at elevated temperatures and imparting stable COF high temperature. Also, it improves thermal conductivity [6] and consequently decreases the contact temperatures over severe braking conditions [11–13].

Throughout the literature, there has been an attempt to reach a Copper-Free formulation with just one ingredient as a possible alternative for

copper [14]. But replacing copper just with one component is an impossible task to achieve. For instance, Bijwe et. al. [15] incorporated a particular type of graphite into the formulation known as thermo-graphite (TG). The outcome revealed that thermo-graphite could be considered as a replacement for copper in some aspects, such as thermal conductivity and lubricity. But using TG, more than 10% affect the mechanical properties, COF stability, and fade resistance in an undesirable way.

To achieve a suitable Copper-Free formulation, at least two ingredients must be used [16, 17]. Tavangar et al. [16] have recently reported copper substitution using TG and cellulose into the composite that improved wear resistance and increased friction stability. However, in the case of friction recovery and thermal resistance compared to the FC containing copper, there is still a need to improve once the replacement is made. Bijwe et al. [18] investigated the influence of Nano-Potassium Titanate (NKT) on the NAO FC. They stated that Nano-KT particles improved the stability of the COF and enhanced the wear resistance. In another study done by Jang et al. [19], they studied the synergistic effects of phenolic resin (high and low molecular weight) and Potassium Titanate in the form of platelets and whiskers. They found out that the friction and wear performance improved with high molecular weight and platy Potassium Titanate due to the large plateaus on the sliding surface.

A man-made vitreous fiber (MMVF, inorganic synthetic fiber, or ceramic fiber) has been used to replace natural asbestos mineral fibers by Han et al. [20] showed that the fade resistance of friction material significantly improved. Ceramic fibers usually can be classified into vitreous fibers, monocrytalline fibers, and polycrytalline fibers. MMVFs with a high melting point is historically produced as thermal insulator. Ming et al. [21] studied the tribological and thermal

characteristics of the combination of potassium titanate whiskers (PTW) with ceramic fiber. They brought about that both materials played a crucial role in the higher friction stability and the wear resistance in the different conditions. However, PTW is not entirely free of risks and is under investigation as potential mesothelioma and possibly carcinogenic to humans [22]. It was also found that the larger the specific area was, the better the fade-recovery characteristics such that the morphology of potassium titanate imparts a big difference on friction composite tribological properties. The platy form has shown a lower wear rate and good friction stability at high temperatures [23]. Wrapping up all statements made above, there has been no report dealing with the combined effect of the MMVF and Potassium Titanate on the performance of Copper-Free brake pads. In that sense, this work is directed towards developing brake pad formulation by substituting copper with the simultaneous use of Potassium Titanate Platelets (PTP) and anti-high temperature ceramic fibers (CFs) in the research and development center of Ettihad Lent Pishro Sanat (ELPS) company- Iran. The friction performance procedures were conducted to study the tribological behavior and wear mechanism of Copper-Free friction material containing PTP, and CFs (hereinafter C0) compared to a commercialized copper-contain friction composite with 7% copper (from now on C7). The fade and recovery and wear tests were discussed using thermal analysis and microstructural characterization techniques.

## 2. EXPERIMENTAL PROCEDURES

### 2.1. Material and methodology

Table 1 shows the PTP specification used in this research. This study's ceramic fiber was short fiber with an average length of 1.5-2 mm and an average diameter of 3-15  $\mu\text{m}$ , Table 2.

**Table 1.** Specification of potassium titanate platelet (PTP)

Properties	PTP	Test method
pH	9-12	
Moisture, %	<0.6	
Bulk density, g/cm <sup>3</sup>	0.5-0.9	
Medium size, $\mu\text{m}$	5-12	Laser diffraction
Surface area, m <sup>2</sup> /g	2-5	BET
Chemical composition, %	TiO <sub>2</sub> : 65-75 K <sub>2</sub> O: 17-22	Chemical Analysis, XRF

**Table 2.** Specifications of ceramic fiber (CF)

Properties	Ceramic Fiber (FC)
Moisture, %	<1.0%
Shot content, %	<0.5
Ignition loss, %	<3
Density, g/cm <sup>3</sup>	0.2-1.9
Mohs hardness	5-6
Main diameter, μm	3-15
Main length, μm	1500-2000

**2.2. Development of FC**

Copper-Free formulation, C0, was developed, and its tribological characteristics have been compared with a commercial copper contained, C7. Table 3 shows the two semi-metallic friction materials with 67% parent composition and 7% copper and alternative materials. The amount of

ceramic fiber and Potassium Titanate platelets and their ratio in the C0 formulation have been briefly reported because of confidential reasons.

Figure 1 shows the process flow for brake pad production that includes; dry mixing, pre-forming, hot pressing, heat treatment or baking, grinding, and painting. Friction materials were mixed in a home-made plough shear mixer at 3600 rpm for 10 min.

Fiber opening or fibrization must be carried out exclusively to make it into uniform fiber length in a high-speed lodge with chopper speeds as high as 3000 rpm [24]. Therefore, fiber-like ingredients were initially loaded into the mixer with barite powder and mixed for 3 minutes before other ingredients were added. The detail of the mixing operation is as such brought in Table 4.

**Table 3.** List of friction composite formulation ingredients.

Friction Material	C7 [wt.%]	C0 [wt.%]
Main ingredients Binder: phenolic resin, rubber Reinforcement: steel fiber, aramid pulp Filler: vermiculite, calcium hydroxide, mica friction modifier: Alumina, flakegraphite, magnesium oxide, coke, antimony	67	67
Barite	Bal.	Bal.
Copper fiber	7	--
Ceramic Fiber (CF)	--	7
Potassium Titanate Platelet (PTP)	--	--

**Table 4.** Mixing sequence of ingredients in the home-made plough shear mixer.

Batch no	Ingredients	Mixing Time (min)	On/Off
1	Aramid pulp, Ceramic fiber, Steel fiber, Barite	3	Chopper
2	Vermiculite, Calcium hydroxide, Mica, Alumina, Magnesium oxide	2	-
3	Phenolic resin, Rubber, Flake graphite, Antimony, Coke	1	-
All Batches		2	Chopper

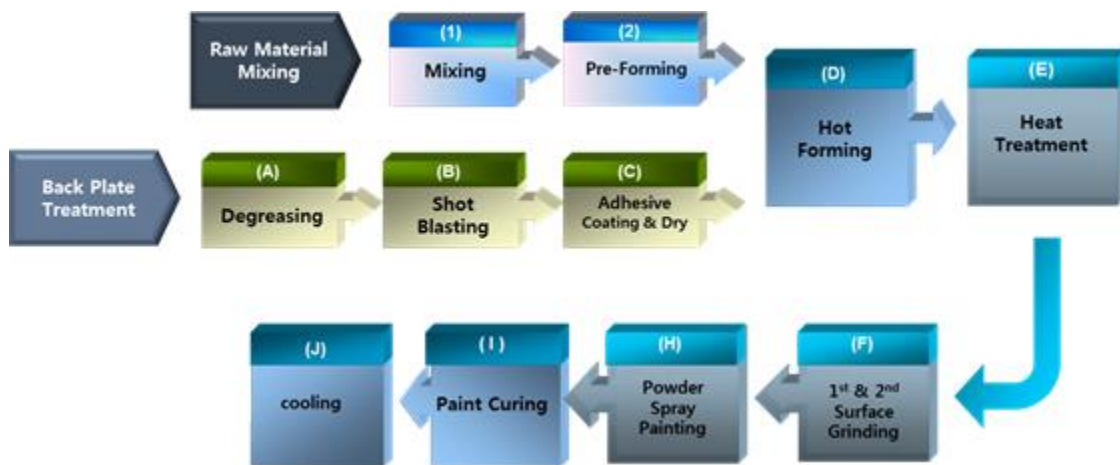


**Fig. 1.** Preparation process of brake pad sample.

### 2.3. Physical and mechanical characterizations

The main physical properties of the as-fabricated pads, such as apparent density and porosity, were measured based on the Archimedes method, according to JIS D4418 using a Sartorius balance with 0.1mg resolution. At least three samples were measured, and the average value was reported with associated uncertainty within 95% of the confidence level. Thermal Gravimetric Analysis, TGA, and Differential Thermal Analysis, DTA (STA, Bahr, Germany) were carried out under the ambient atmosphere at the heating rate of 10°C/min to evaluate the thermal stability of FCs. The loss on ignition (LOI) of the friction material was calculated by weighing the friction powders before and after thermal analysis, and the difference is reported as a percent.

The mechanical properties in the form of hardness were measured using a Rockwell hardness machine

(INNOVA TEST, Netherland) in R-scale as per ASTM E8 standard practice. At least five measurements were made, and the average value was reported with an uncertainty of  $\pm 2$  HRR within a confidence level of 95%.

### 2.4. Performance test on chase dynamometer

The friction and wear behaviors of the friction composites were performed using a Chase Dynamometer according to the SAE J661 standard. The specimens were cut to a dimension of 25.4 square pads with 6 mm thickness and then pressed against the inner diameter of the brake drum of the Chase dynamometer, shown schematically in Figure 2. The rotating brake drum is made of pearlitic grey cast iron, similar to the brake disc. A k-type calibrated thermocouple was used to record the temperature during the test within  $\pm 1^\circ\text{C}$  uncertainty.

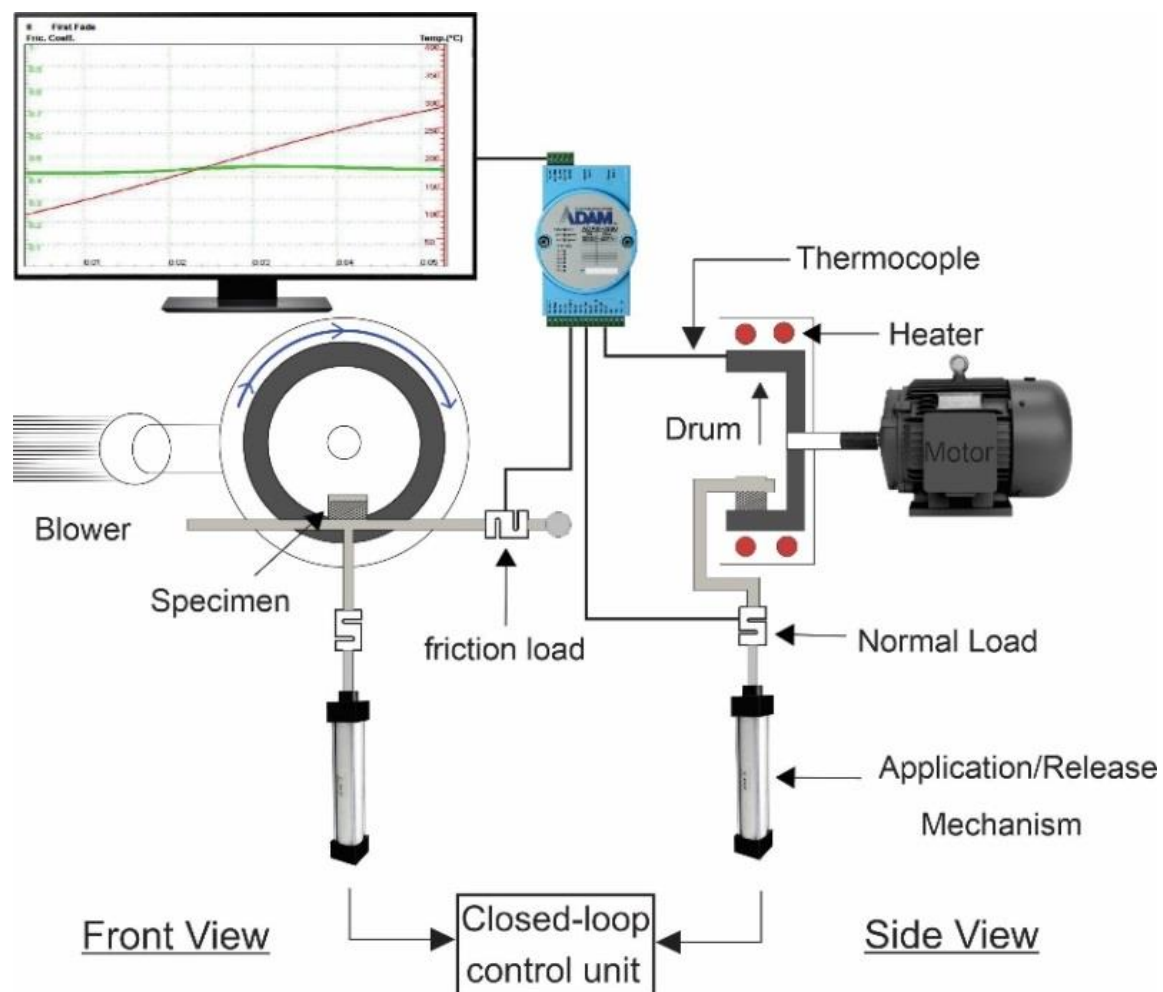


Fig. 2. Schematic representation of the friction test device (Chase dynamometer).

The standard procedure consists of the burnishing process and subsequent stages as reset, baseline, first fade, first recovery, wear, second fade, second recovery, and baseline rerun. All test procedure parameters correspond to the SAE-J661 test standard, which is given in Table 5.

The friction test samples were weighed before and after the performance test. The material loss from the sample surface is measured using an electronic balance with a resolution of 0.1 mg (Ohaus, PA413C model). The wear (w) is expressed as in terms of the specific wear rate (SW) or the wear factor according to the following relation:

$$\% S.W = \frac{\Delta m}{\rho \times \Delta s \times F_N}$$

Where S. Wis the specific wear rate in m<sup>3</sup>/N.m, Δm is the mass loss of the specimen in gram by weighing the specimen before and after the test, ρ is the density of the specimen in g/m<sup>3</sup>, Δs is the sliding distance in meter measured upon braking, and FN is the applied normal force on the sample in Newton. Three measurements were made, and the average value was reported with associated uncertainty within a confidence level of 95%.

### 2.5. Characterization of the worn surface

The worn surfaces of friction samples after the performance test were studied using the scanning electron microscope (TESCAN VEGA//XMU

SEM) equipped with X-ray map analysis.

## 3. RESULTS AND DISCUSSIONS

### 3.1. Physical, mechanical, and thermal characterization

Figure 3 presents CF's morphology, supplied by Jiansu REK High-Tec Materials Co. and PTP, provided by Nantong Auxin Electronic Technology Co.

The chemical composition of mineral fibers varies significantly from one geographical region to another, fiber length distribution was not under control, and many non-fibrous species, usually called shots, beads, or slugs, are present. Particular attention must be paid to shots in fibers since shots are generally hard and brittle particles. Table 6 shows the physical and mechanical properties of two typical brake pads made from two different formulations. The reduction in the specific density of C0 is due to the lower densities of CF and PTP compared to copper. However, the porosity and hardness are kept almost unchanged, given they are functional properties of the brake pads related to the process parameters such as pressure, temperature, and time.

The comparison of the LOI for C0 with that of C7 shows a lower amount of degradation over thermal analysis translated into a better thermal resistance during service depending on the braking conditions of vehicles given the temperature of pad surface may reach 500°C.

**Table 5.** Chase testing schedules according to SAE J661.

Stage	Speed (rpm)	Temperature (°C)		Load (N)	ON time (s)	OFF time (s)	Application	On/Off
		Min	Max					
Burnishing	312		93	440	1200	-	1	
First baseline	417	82	93	667	10	20	20	
First fade	417	82	288	667	600	-	1	Heater
First recovery	417	260	93	667	10	rest	1	Blower
Wear	417	193	204	667	20	10	100	
Second fade	417	93	345	667	600	-	1	Heater
Second Recovery	417	317	93	667	10	rest	1	Blower
Second baseline	417	93	93	667	10	20	20	

**Table 6.** Physical and mechanical properties of the brake pads.

Friction composite	Porosity [%]	Specific gravity (g/cm <sup>3</sup> )	Hardness (HRR)	LOI (%)
C0	12.5±0.5	2.40±0.01	95±2	15
C7	11.5±0.5	2.58±0.01	92±2	19

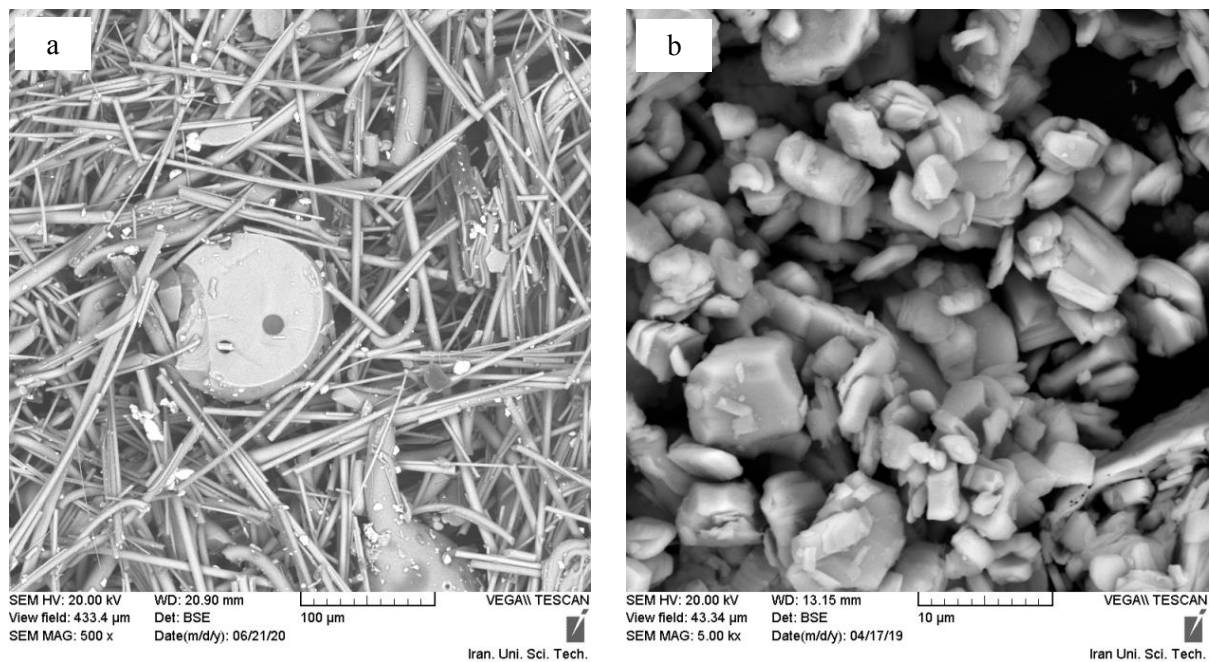


**Fig. 3.** SEM micrograph of (a): Ceramic fiber and (b): Potassium titanate platelet.

In order to have a better comparison of the thermal behavior of C0 and C7 FCs, thermal analysis was carried out, and the outcomes are shown in Figure 4.

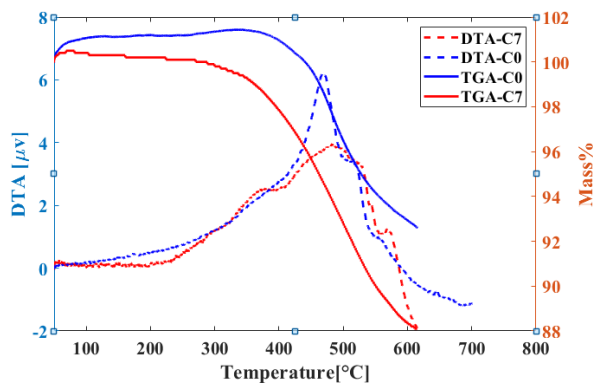


**Fig. 4.** Comparison of C0 and C7 thermal behavior curve, heating rate 10°C.

The TGA curve indicates that C0's thermal behavior offers better stability over temperatures in comparison with C7. The more stability of C0 at elevated temperature can be attributed to PTP and CF, which caused an enhancement in thermal resistance and led to postponing the degradation point of phenolic resin to a higher temperature. PTP has a melting temperature near copper, and the melting point of CF is around 1800°C. In Figure.4, C0 has shown a perceptible decrease in weight started at about 450°C, whereas in C7,

degradation starts at around 300°C with a difference of 150 units. The high thermal stability of PTP and CF can shift the degradation point of less thermal resistance ingredients to a higher temperature, which leads to the better thermal resistance of an FC. In other words, the friction composite containing CF and PTP exhibited more stable thermal behavior attributed directly to the synergistic effect of CF and PTP in the friction composite.

The CF caused an enhancement of thermal stability led by the strengthening of PTP as the inter-molecular interaction between phenolic resin-based matrix and CF and PTP [21]. At the end of the thermal analysis, the amount of mass loss differs in favor of the C0 (7.5% mass loss for C0 and 12% for C7) that resulting in a lower wear rate of C0. As mentioned earlier, PTP has a melting point near the copper. A laminar crystal structure is a suitable choice for a high-temperature modifier, which reduces the wear rate at elevated temperatures and increases COF stability [17].

Multistep mass-loss with exothermic peaks between 230-600°C shows a large exothermic peak for both FCs corresponds to the decomposition of phenolic resin, followed by two small exothermic peaks correspond to the combustion of carbonaceous ingredients within the two formulations [25].

### 3.2. Tribological behavior

Figure 5 represents the two crucial stages of friction evaluation according to the SAE J661 standard known as the fade and recovery stages. Each one has two levels named moderate (first) and severe (second) conditions. During the fade period, the moderate level runs continuous drag for 10 min, or until 288°C is attained, any state is met first. After the first fade, the recovery stage was completed with an immediate turning-on the cooling system and COF measured at four different temperatures (260, 204, 149, and 93°C). At the fade stage's severe level, there is a continuous drag for 10 min or until drum temperature reaches 343°C. The intense level for recovery level of the severe condition starts immediately after the fade, but this time the COF was measured at 316, 260, 204, 149, and 93°C. The COF against pad brakings are shown for the two conditions are gathered in Figure 5.

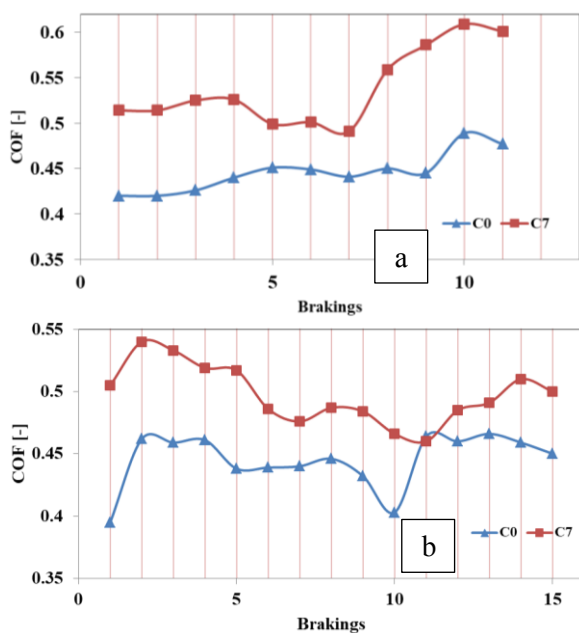


Fig. 5. The COF as a function of temperature, a) moderate condition and b) severe condition.

Frictional characteristics of C0 and C7 friction composites show a similar trend as a function of temperature. With increasing brake pad temperature, the COF decrease, and decrement in temperature leads to COF enhancement. On the one hand, C0 represents more stability in the COF variation when compared to C7 and, on the other hand, a mild COF, i.e., between 0.35-0.45, brings about enhancing the lifetime of the brake disk.

One of the significant concerns of achieving a reliable COF is to have moderate COF with the lowest oscillation. In both test conditions, C0 represents a more stable COF and less oscillation, which leads to comfort braking during service.

The incorporation of CF into the formulation strongly promoted the brake pad's fade resistance and recovery performances. According to Figure 5a, at moderate conditions, In fact, the COF increases slightly until a maximum temperature of 288°C is reached. Han et al. [20] reported that using CF up to 5wt% in the FC increases the fade and recovery performance for the benefit of COF and wear rate stability. Therefore, the amount used for the C0 composite has shown a suitable trade-off between stability and fade-recovery performance.

As stated earlier, PTP reacts with phenolic resins, thereby effectively accelerate resin decomposition into the lower residue around the asperity, which is created by the deterioration of resins under frictional heat build-up [26]. Thus, Titanates cannot play the role of lubricant or abrasive material within the formulation, but rather as friction modifiers that help the formation of uniform friction film upon contact plateaus (CPs), which leads to both continuous contact and smooth friction[27], [28]. Figure 6 depicts a schematic diagram of how PTP plays its role around the asperities.

To get a better insight into the variation of the COF over the fade, recovery, and wear runs in the moderate and severe conditions, three ratios are defined as fade, recovery, and wear ratio (in %):

$$\% \text{Fade Ratio (FR)} = \frac{\mu_{\min}}{\mu_{\max}} \times 100$$

$$\% \text{Recovery Ratio (RR)} = \frac{\mu_{\min}}{\mu_{\max}} \times 100$$

$$\% \text{Wear Ratio (WR)} = \frac{\mu_{\min}}{\mu_{\max}} \times 100$$

where  $\mu_{\min}$  is the lowest and  $\mu_{\max}$  is the highest COF collected during test performance of moderate and severe conditions. To achieve the optimum friction performance, the highest ratio is desirable that means the difference between  $\mu_{\max}$  and  $\mu_{\min}$  should be as small as possible. Calculated tribological ratios out of the equations mentioned above and the experimental data in Figure 5 have been tabulated in Table 7.

At moderate conditions, the fade performance of C0 shows a promising result,  $FRC_0 > FRC_7$  while, recovery behavior presents a similar manner,  $RRC_0 \approx RRC_7$  between the two formulations.

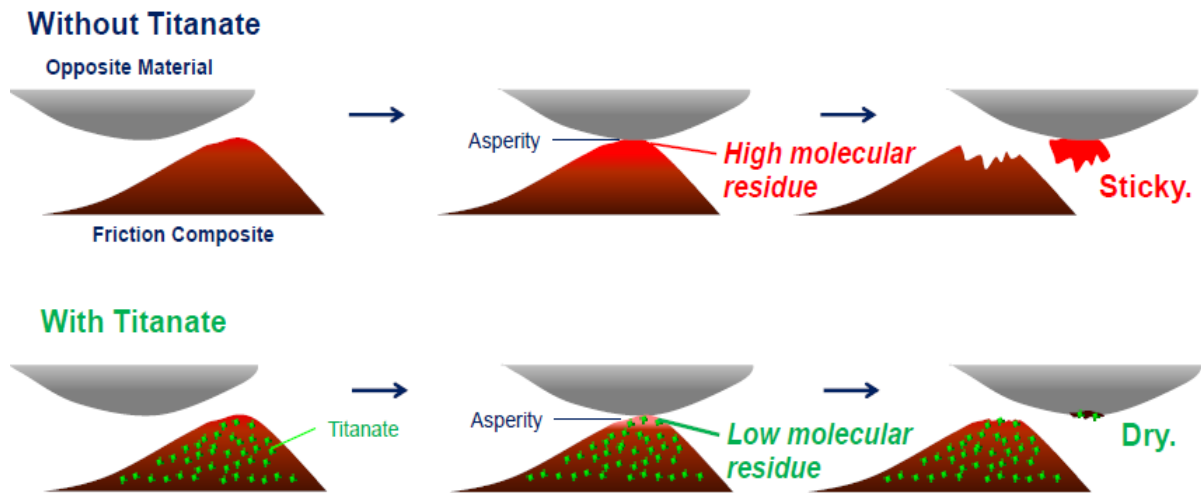


Fig. 6. General function of PTP benefits around asperities.

Table 7. Fade and recovery ratio data of C0 and C7 friction composite.

Friction composite	Moderate condition		Severe condition	
	FR	RR	FR	RR
C0	107	92	87	97
C7	93	93	86	90

During the severe condition, fade ratios for two materials were in the same order:  $FRC0 \approx FRC7$  and recovery performance are more for C0, i.e.,  $RRC0 > RRC7$ . PTP and CF's synergetic effect clearly shows itself during severe conditions, which imparts more stability to the COF and better recovery ( $RRC0 > RRC7$ ). Over the wide range of temperatures and brakings, Table 6 clearly shows the superiority of C0 versus C7.

The variation of COF during wear run has illustrated in Figure 7a. According to the equation for wear ratio, the values for C0 and C7 were calculated as 89% and 92%, respectively. The closely the same proportions may imply that COF's stability in the wear run for C0 and C7 is almost the same. Smoothing techniques like moving average reduce the two data series' volatility, identifying significant tribological trends.

The moving average of COF during the wear run is shown in Figure 8b. One can easily argue that C0 has an ascending trend line as a function of the braking number. On the contrary, C7 illustrates a descending trend line during wear runs. Both FCs have good stability, but C0 keeps its frictional performance during long braking cycles, meaning better braking during service.

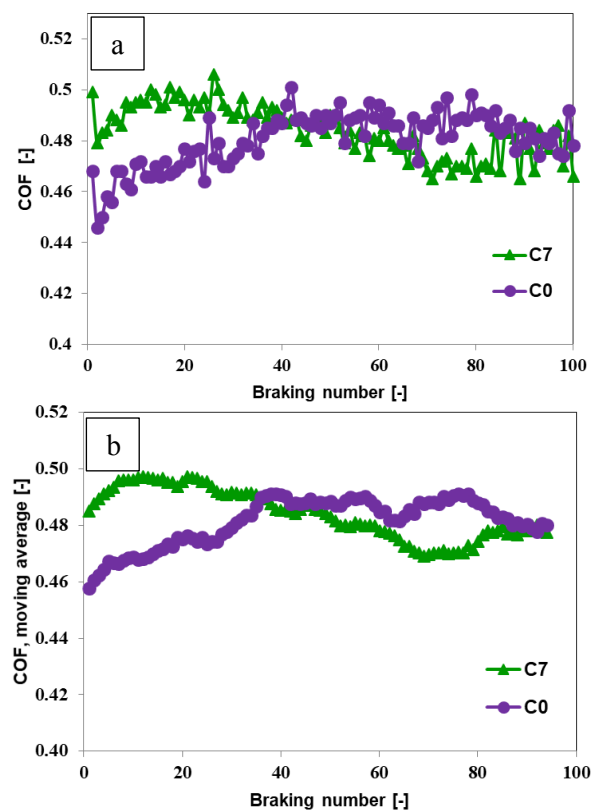
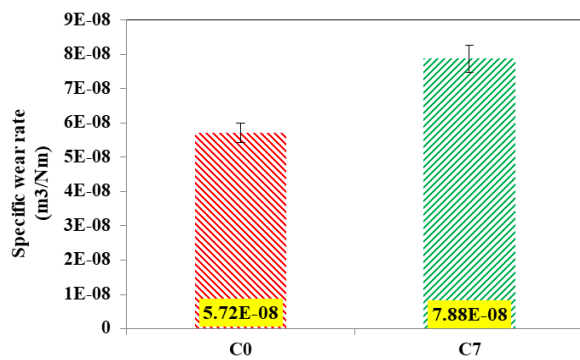


Fig. 7. (a) The COF as a function braking number in wear test for the C7 and the C0 friction composites and (b) moving average curve.



**Fig. 8.** Specific wear characterization of the two friction composites.

The wear rate was expressed in terms of specific wear rate (SW) after completing the friction test, and Figure 8 compares this parameter for C0 and C7 formulations. After having said all above, it is not surprising that C0 possesses better wear resistance due to the alteration of wear mechanism caused by PTP and CF, although they are in the same order of magnitude.

### 3.3. Wear mechanism

#### 3.3.1. Worn surface analysis

Figure 9 shows the SEM micrographs of the worn surface of the FCs. Generally speaking, the contact plateaus (CPs) formed during the sliding of FC against the disc rotor dictate the tribological performances, such as COF level, noise, vibration, fade, recovery [29].

The worn surface of C0 is composed of more secondary contact plateaus (SCPs) with a large area and better tribological performance than that of C7, Figure 6b. Moreover, it showed a smooth topography and thin film with some cracks due to the brittle behavior of SCPs.

In a copper-containing friction material, the tribological behavior rests on copper's role in forming the CPs and friction film discussed thoroughly [16]. However, the role of PTP on the tribological characteristics of CPs and friction film is not appropriately defined. Ho et al. [30] illustrated potassium titanate platelets' effect on the formation of CPs well below 350°C temperature.

The study concluded that PTP promotes the formation of SCPs, led the brake pad to wear resistance better. Thereby, the large SCPs on the worn surface shown in Figure 9a promoted the stability of friction film, led to COF stability, and, as a result, lead to a lower wear rate.

To assess the main ingredients' distribution on the worn surface, Figure 10 presents the elemental X-ray maps of the C0 worn surface. Iron distribution in Figure 10b, as anticipated, indicates the role of steel fiber in the formation of primary contact plateaus (PCPs). The steel fibers possess high wear resistance and act as nucleation sites for the growth of SCPs [31].

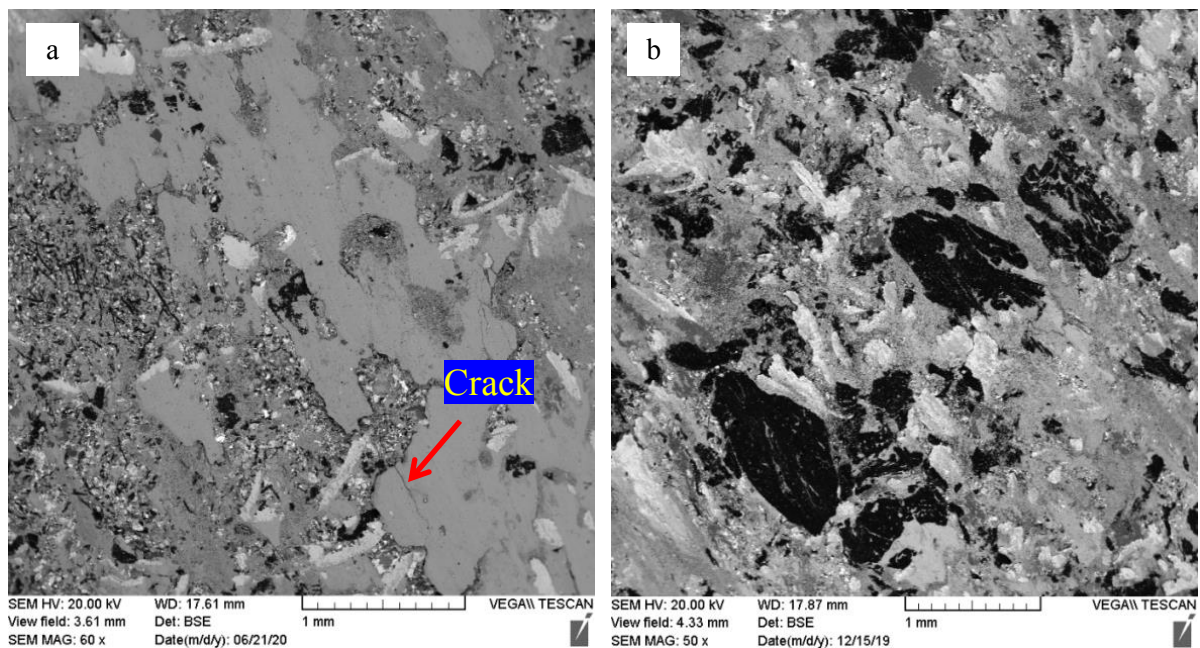


**Fig. 9.** SEM of the worn surface micrograph of a) C0 and b) C7.

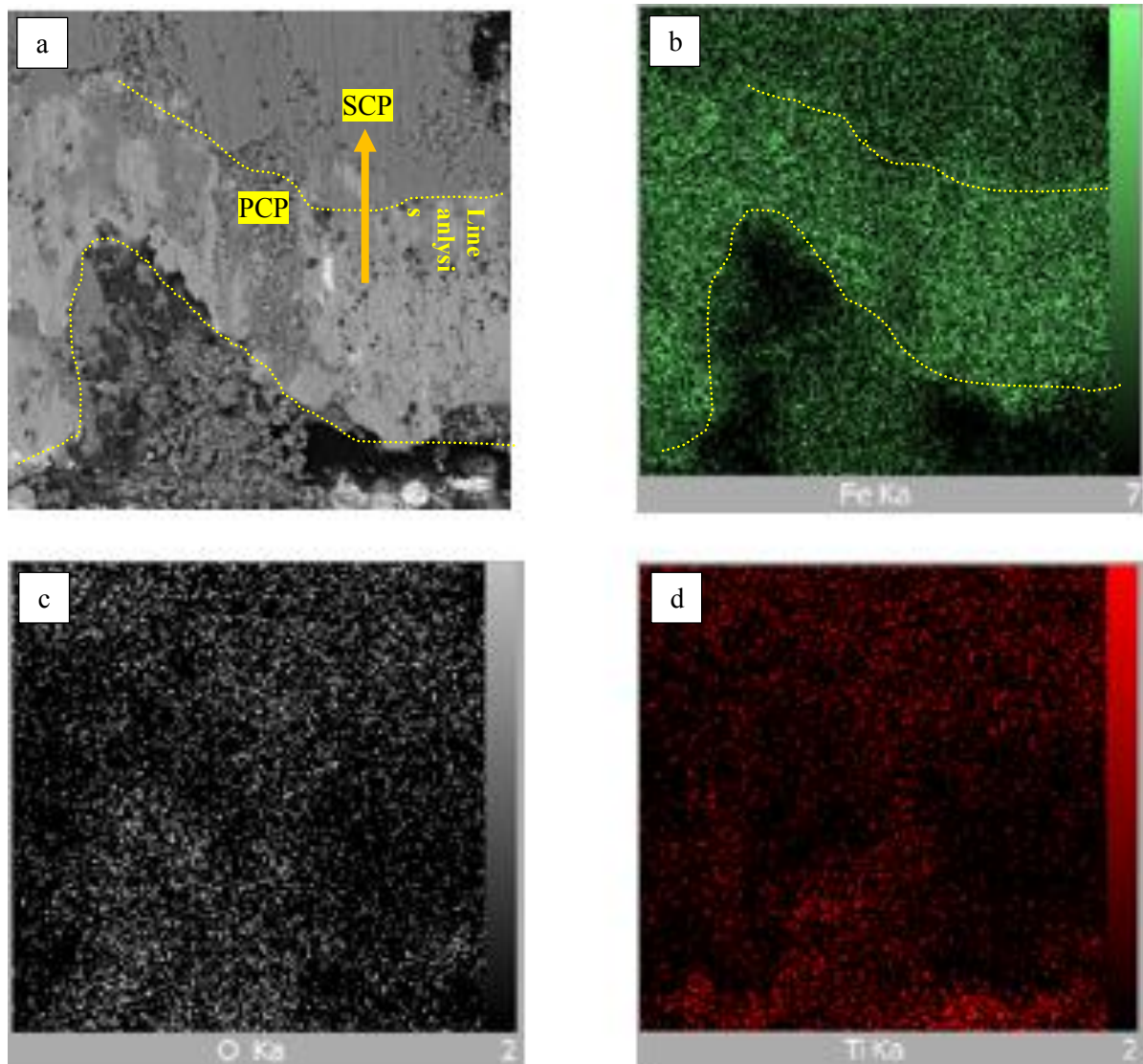


**Fig. 10.** Elemental mapping of C0 worn surface, a) main micrograph and the arrow represent the line analysis location, b) Fe in green, c) O in white, d) Ti in red.

In the case of oxygen, it is more frequently distributed upon CPs as contacts surface, resulting from oxides formation during brake application. The uniform distribution of Ti upon the SCPs shown in Figure 10 d confirms the effect of PTP on the formation of SCPs and their stability at elevated temperatures that lead to less oscillation of COF in the different braking situations.

The role of different elements in forming primary and secondary contact plateaus is assessed through the X-ray line profile analysis of Ti, K, Fe, and O shown in Figure 11. Passing through the primary region into the secondary region, the amount of titanium and oxygen increased.

As a general fact, the worn surface's morphology

dynamically changes during the braking service and makes different morphology of the worn surface. To achieve a friction composite showing a stable tribological performance at different braking conditions, it must include materials to facilitate reliable CPs on the worn surface.

At the same time, it should possess good thermal properties to withstand high-temperature conditions. Thereby, a combination of PTP with CF maintains the CPs at different temperatures bringing about more thermal stability at elevated temperatures.

The variation of oxygen and iron across the CPs reveals the moving from the primary plateau to the secondary one, the amount of Fe decreased while oxygen increases. This is the fact that the

steel wool within the formulation is playing the primary role in forming the primary contact plateau while more oxygen upon the SCP represents jammed and piles up of oxide debris against the PCPs.

Figure 12 presents the X-ray maps for a different combination of Fe, Ti, K, and O upon two CPs of Figure 9. The distribution of Ti upon the SCP in Figure 12a assumes that PTP can bring about forming stable PCPs. It has a great potential to stabilize fade and wear characteristics and create a thin transfer-film that modifies the COF's magnitude. The SCPs are comprised of wear debris, including soft materials and abrasive particles which accumulated behind the PCPs as barriers. In a Chase test, the normal pressure, shear force, and friction can compact the wear debris to form the SCPs [31]. The uniform distribution of Ti and K on the SCP, Figure 12c, helps maintain the SCPs at different braking conditions, especially at elevated temperatures, and overcomes the real concern of the brake pad designers to have more stability in COF [28], [32], [33].

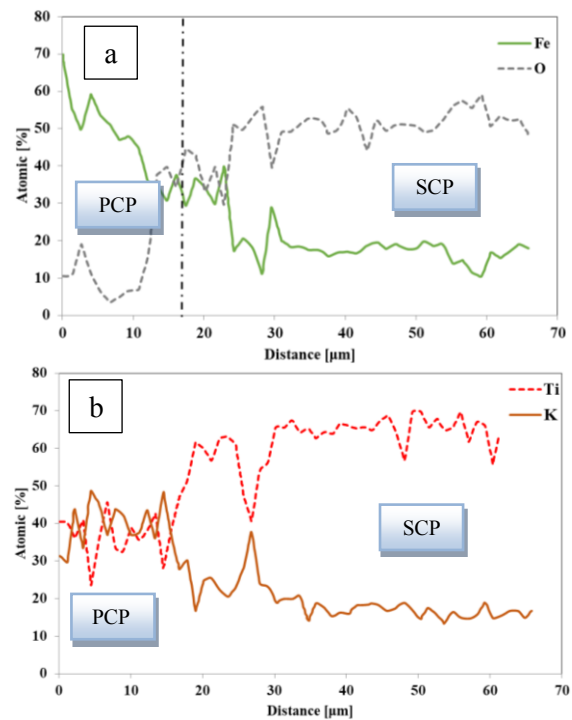


Fig. 11. X-Ray line profile analysis of main elements affecting the wear mechanism upon CPs, a) Fe and O and b) Ti and K.

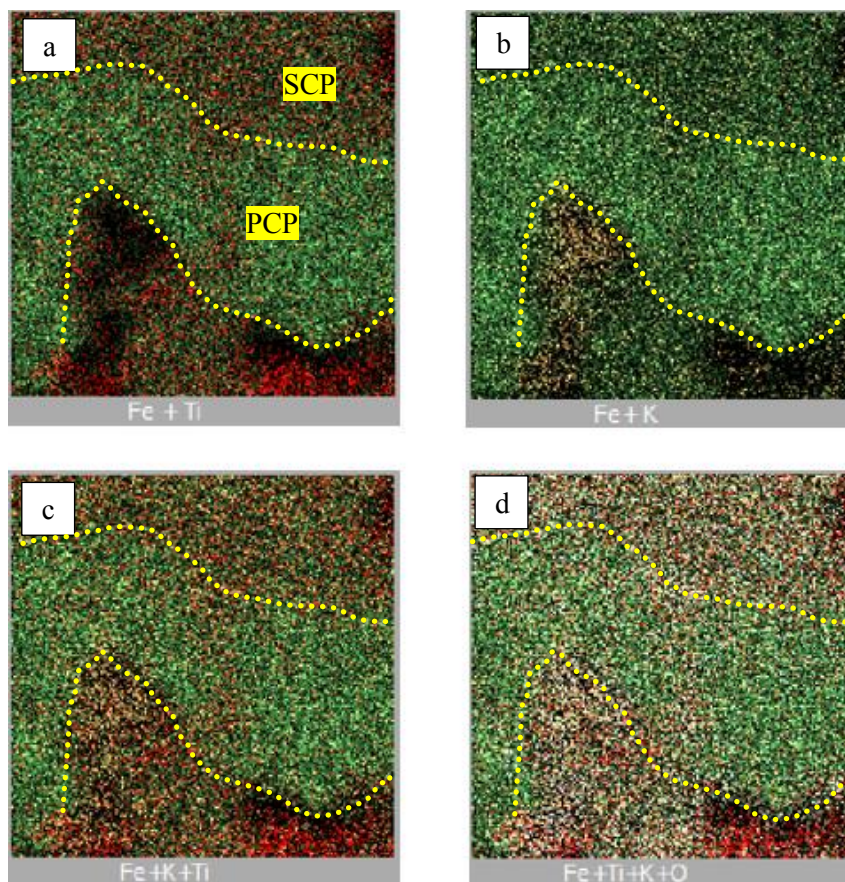
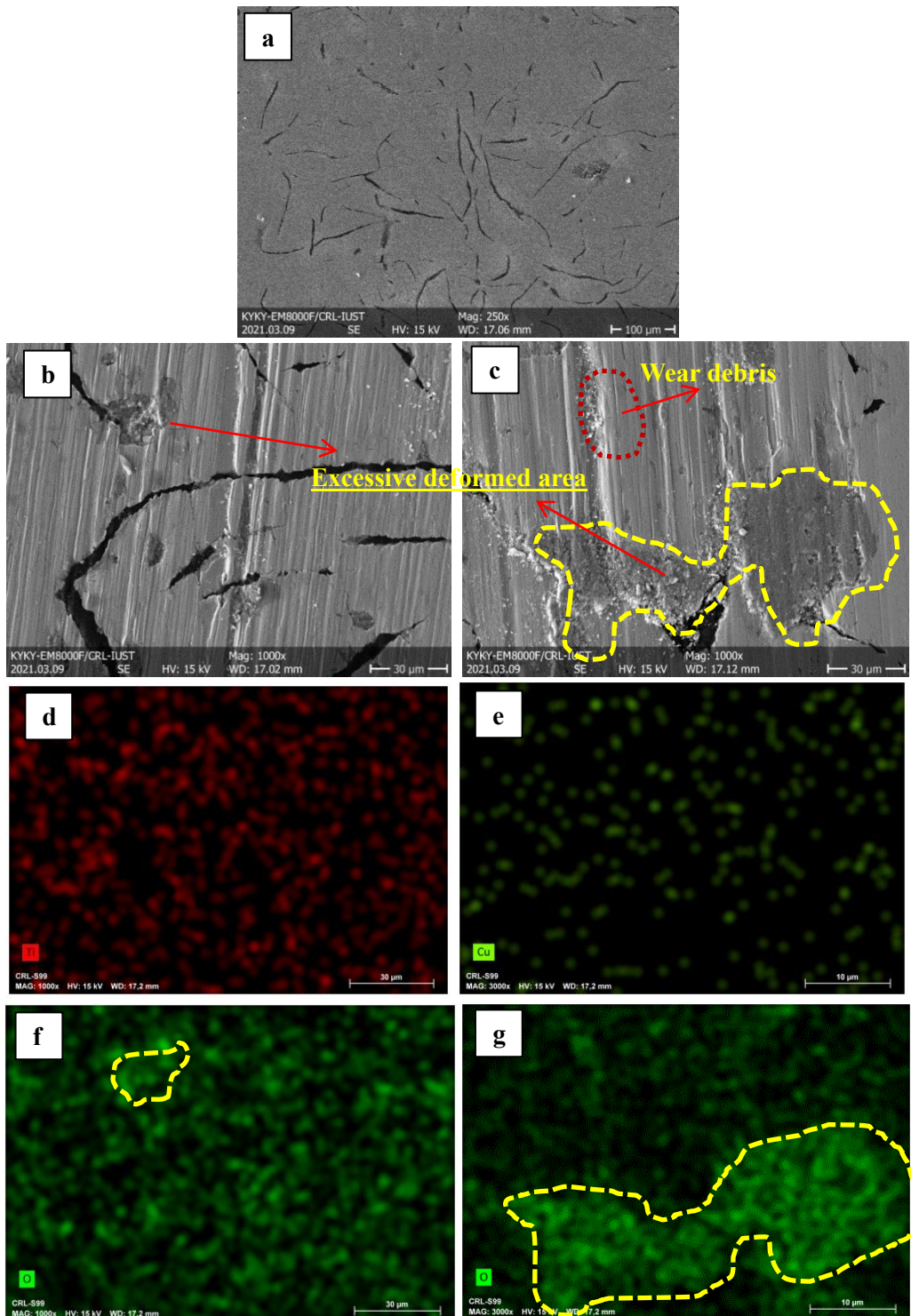


Fig. 12. EM combination of main elements, a) Fe + Ti, b) Fe + K, c) Fe + K + Ti, and d) Fe + K + Ti + O.



**Fig. 13.** SEM images of disc surface after wear test: (a) microstructure of The Grey cast iron, (b) wear track of the disc against the C0 pad, (c) worn surface of the disc against the C7 pad, (d) and (f), X-ray elemental distribution of Ti and Oxygen on Brake disc against C0 brake pad, (e) and (g) X-ray elemental distribution of Ti and Oxygen on Brake disc against C0 brake pad.

Figure 12d, finally, shows all elements together, describing that steel fiber has a primary role in forming both PCPs and SCPs. On the other hand,

Figure 13a depicts the microstructure of the grey cast-iron of the brake disc and Figures 13b and 13c represent the wear track of two counterparts

cast-iron disc against C0 and C7 friction pad composites, respectively.

Due to abrasive materials such as alumina and steel fibers in brake pads, the sliding disc's worn surface is composed of grooves and excessive deformed areas. However, as already stated, copper can strongly promote the formation of friction film between a pad and its counterpart disc surface. Having omitted copper from the pad's composition, PTP can be used to maintain the friction film's stability as its melting point is relatively close to that of the copper and with a lamellar crystal structure [17]. The scanning electron microscopy observation on the Titanium bearing and copper-bearing distributions on the associated discs implies the PTP, as a friction modifier, can play a significant role in maintaining the friction film created between the brake disc surface and the friction surfaces of the brake pad, shown in Figure 13d and 13e.

Furthermore, upon Figures 13f and 13g, one can readily conclude that the disc underwent severe abrasive wear led to oxidization on the disc surfaces. But, the more excessive deformation, the more oxidation happens during sliding. This in-and-of-itself reduces the stability of the friction film formation, and the model shown in

Figure 6 can be validated when a brake pad contains PTP. Daimon et al. [26] studied the interaction between the titanate compounds and the phenolic resin. They have found out that titanate causes a chemical change in the cross-linked resin under high temperatures such that under braking lesser amount of debris is produced. This reaction can make a stabilized and uniform friction film between the brake pad and its counterbody brake disc. The schematic diagram shown in Figure 14 represents the idea of changing the friction behavior when the titanate is added to the phenolic resin-bearing friction composite. Accordingly, it leads to a decrease in wear debris, which increases the effective lifetime of friction film on the stability of COF [16].

#### 4. CONCLUSIONS

This work was based on comparing a copper-bearing brake pad formulation and a formulation containing potassium titanate platelets (PTP) and a particular ceramic fiber (CF). The effect of these elements on the stability of COF and friction performance such as fade and recovery performance was also studied, out of which the following conclusions can be drawn:

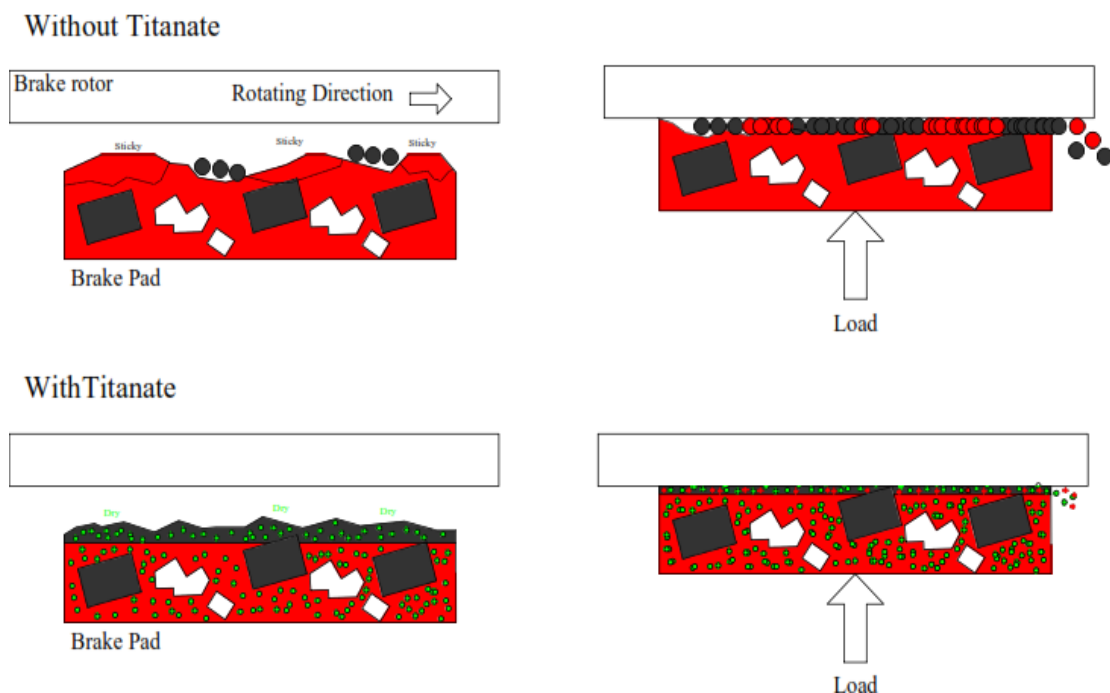


Fig. 14. effect of PTP on wear mechanism and formation of stable SCPs.

- The incorporation of PTP, together with CF into the friction material formulation, has shown reliable and stable COF over high-temperature braking compared to the copper contacting friction material composite. PTP and CF's synergetic effect brought about better fade resistance, low wear rate, and optimum COF of a brake pad against its brake disc counterpart.
- The contribution of PTP as a high-temperature modifier and its effect on the nature of the cross-linked phenolic resin on the mating surface around asperities provided continuous secondary contact plateaus and smooth friction. Thus, PTP plays a crucial role in forming a uniform thin transfer film upon the contact plateaus.
- The participation of CF as anti-high temperature fiber enhanced the friction composite's thermal behavior that made the proposed formulation a suitable choice for vehicles.

## 5. ACKNOWLEDGMENT

The authors are grateful to the staff members of ELPS Co.: Mr. M. R. Riazalhosseini, Mr. S. Drikvandi, (ELPS brake Co.'s staff) for their real help during the experimental procedures of this study. Also, the authors are grateful to Otsuka Chemical Co., Ltd. for providing helpful information about use of potassium titanate in the friction materials.

## REFERENCES

- [1] Cox. L. R., Engineered Tribological Composites: The art of friction material development. SAE; 2012. Warrendale, USA, PA 15096-0001.
- [2] Kumar, V., Kumaran, S, "Friction material composite: types of brake friction material formulations and effects of various ingredients on brake performance—a review" Mater. Res. Express, 2019, 6, 325-365.
- [3] Bonfanti, A., "Low-impact friction materials for brake pads" Doctoral dissertation, University of Trento, 2016, 353-382.
- [4] Bijwe, J., "Composites as friction materials: Recent developments in non-asbestos fiber reinforced friction materials a review," Polym. Composite., 1991, 18, 378–396.
- [5] Chan, D. and Stachowiak, G. W., "Review of automotive brake friction materials," Proc. Inst. Mech. Eng. Part D J. Automob. Eng., 2004, 218, 953–966.
- [6] Österle, W., Prietzel, C., Kloß, H. and Dmitriev, A., "On the role of copper in brake friction materials," Tribol. Int.-TRIBOL INT, 2010, 43, 2317–2326.
- [7] Barros, L., Poletto, J., Neis, P., Ferreira, N. F. and Pereira, C., "Influence of copper on automotive brake performance," Wear, 2019, 426, 741–749.
- [8] Kim S. J., Lee J. Y., Han J. M., Kim Y. C., Park H. D., Sung S. H., Lee J. J., Cha J. H., Jo J. H., Jang H., "The role of copper on the friction and wear performance of automotive brake friction materials," SAE International Journal of Materials and Manufacturing. 2012, 5, 9-18.
- [9] Straffelini, G., Ciudin, R., Ciotti, A. and Gialanella, S., "Present knowledge and perspectives on the role of copper in brake materials and related environmental issues: A critical assessment," Environ. Pollut., 2015, 207, 211–219.
- [10] Kumar M. and Bijwe, J., "Non-asbestos organic (NAO) friction composites: Role of copper; its shape and amount," Wear, 2011, 270, 269–280.
- [11] Lee, P. W. and Filip, P., "Friction and wear of Cu-free and Sb-free environmental friendly automotive brake materials," Wear, 2013, 302, 1404–1413.
- [12] Lee, P. W., Leist, J. and Filip, P., "Use of Hexagonal Boron Nitride in Automotive Friction Materials," SAE Technical Paper, 2010, 311, 218-229.
- [13] Cho, M., Ju, J., Kim, S. J. and Jang, H., "Tribological properties of solid lubricants (graphite, Sb<sub>2</sub>S<sub>3</sub>, MoS<sub>2</sub>) for automotive brake friction materials," Wear, 2006, 260, 855–860.
- [14] Menapace, C., Leonardi, M., Matějka, V., Gialanella, S. and Straffelini, G., "Dry sliding behavior and friction layer formation in copper-free barite containing friction materials," Wear, 2018, 398 191–200.
- [15] Neelamegam, A. and Bijwe, J., "Special

- grade of graphite in NAO friction materials for possible replacement of copper," *Wear*, 2015, 231, 330–331.
- [16] Tavangar, R., Moghadam, H. A., Khavandi, A. and Banaeifar, S., "Comparison of dry sliding behavior and wear mechanism of low metallic and copper-free brake pads," *Tribol. Int.*, 2020, 151, 406–416.
- [17] Mitsumoto, M., "Copper Free Brake Pads with Stable Friction Coefficient," *Tribol. Trans.*, 2017, 59, 23–24.
- [18] Mahale, V., Bijwe, J. and Sinha, S. "Influence of nano-potassium titanate particles on the performance of NAO brake-pads," *Wear*, 2017, 376, 727–737.
- [19] Joo, B. S., Jara, D. C., Seo, H. J. and Jang, H., "Influences of the average molecular weight of phenolic resin and potassium titanate morphology on particulate emissions from brake linings," *Wear*, 2020, 450, 203–243.
- [20] Han, Y., Tian, X. and Yin, Y., "Effects of Ceramic Fiber on the Friction Performance of Automotive Brake Lining Materials," *Tribol. Trans.*, 2008, 51, 779–783.
- [21] Wu, Y., Zeng, M., Yu, L. and Fan, L., "Synergistic effect of nano-and micrometer-size ceramic fibers on the tribological and thermal properties of automotive brake lining," *J. Reinf. Plast. Compos.*, 2010, 18, 2732–2743.
- [22] Zaremba, T. and Witkowska, D., "Methods of manufacturing of potassium titanate fibres and whiskers. A review," *Mater. Sci.*, 2010, 28, 321–330
- [23] Cho, K. H., Cho, M. H., Kim, S. J. and Jang, H., "Tribological Properties of Potassium Titanate in the Brake Friction Material; Morphological Effects," *Tribol. Lett.*, 2008, 32, 59–66.
- [24] Sundarkrishnaa, K. L., "Friction material composites.", Springer Berlin Heidelberg, 2012, 31, 52–64.
- [25] Ramousse, S., Høj, J. W. and Sørensen, O. T., "Thermal characterisation of brake pads," *J. Therm. Anal. Calorim.*, 2001, 64, 933–943.
- [26] Daimon, E., Inada, K., Yamamoto, Y. and O'Doherty, J., "Chemical Reaction between Titanate Compounds and Phenolic Resins," SAE Technical Paper, 2011, 20, 23–66.
- [27] Kamifuku, A., Inada, K., Downey, M. and Yamamoto, Y., "The Brake Abrasion Properties in Two Kinds of Platelet Titanate Compound Formulations, and the Swift Brake Property Evaluation by Using the Thrust Test Method," SAE Technical Paper, 2007, 1, 39–50.
- [28] Kamada, S., Inada, K., Downey, M. and Yamamoto, Y., "An Evaluation Method of Brake Pads for New Titanates," SAE Technical Paper, 2009, 35, 30–43.
- [29] Tavangar, R., Moghadam, H. A. and Khavandi, A., "Effect of Steel Fibers on Wear Mechanism of Semi-Metallic Brake Pad Composite," *J. Sci. Technol. Compos.*, 2020, 7, 791–799.
- [30] Jara, D. C. and Jang, H., "Synergistic effects of the ingredients of brake friction materials on friction and wear: A case study on phenolic resin and potassium titanate," *Wear*, 2019, 430, 222–232.
- [31] Eriksson, M. and Jacobson, S., "Tribological surfaces of organic brake pads," *Tribol. Int.*, 2000, 33, 817–827.
- [32] Inada, K., Aki, M. and Yamamoto, Y., "Relationship Between Powder Properties of Titanate Compounds and Brake Performance," *SAE Trans.*, 2005, 114, 3041–3046.
- [33] Kamada, S. and Inada, K., "Effects of Titanates in Low Steel Formulation: Prevention of Metal Pick Up Growth," SAE Technical Paper, 2012, 20, 17–39